



Identification of Shear Modulus Reduction and Damping Curve for Deep and Shallow Sites: Kik-Net Data

Ketan Bajaj and P. Anbazhagan

Department of Civil Engineering, Indian Institute of Science, Bangalore, India

ABSTRACT

Study aims at selecting the suitable shear modulus reduction and damping curve for broad classification of soil, i.e., rock, gravel, sand, and clay. For this purpose, surface and bedrock ground motion recordings from Kik-Net downhole array for both deep and shallow soil sites have been used. Total stress one-dimensional non-linear site-response analysis has been carried out by varying the available curves for a corresponding soil type. Input parameters for few curves have been determined using parametric study. Linear mixed-effect models on residuals from predicted and recorded surface spectra have been used in suggesting the suitable curve for corresponding soil.

ARTICLE HISTORY

Received 16 May 2018
Accepted 30 June 2019

KEYWORDS

Kik-Net; DEEPSOIL; Shear Modulus Reduction and Damping Curve; Site Response; Parametric Study


1. Introduction

Estimation of site amplification due to the local soil is an indispensable part to estimate the level of seismic hazard due to the potential earthquake. Milne [1898] observed the modification in seismic waves as it propagates from the soil stratum. 1987, Mexico earthquake; 1989, the Loma Prieta earthquake; 1995 Kobe earthquake; 2001 Bhuj earthquake; and 2010 Canterbury earthquake are the classic examples that emphasize the influence of site amplification due to the local site effect. Estimation of the dynamic property of in-situ soil deposits is the most significant part in studying the response of soil and structure built on these sites.

Most of the researchers [e.g., Bakir *et al.*, 2002; Hough *et al.*, 2011; Bradley and Cubrinovski, 2011] have concluded that softer materials near the free surface govern the damage pattern at short distances. Various projects (NGA WEST GMPEs project) incorporated site effects using the time average shear wave velocity at 30 m depth. Whereas, in important projects, detailed site-response analysis of the site is performed. In addition to the shear wave velocity profile, strain-dependent shear modulus reduction and damping ratio curves are an essential input parameter to estimate the soil non-linearity response. In the absence of site-specific shear modulus reduction (G/G_{max}) and damping ratio, various authors [e.g., Mahajan *et al.*, 2007; Anbazhagan and Sitharam, 2008; Kumar *et al.*, 2012; Karastathis *et al.*, 2010] have carried out site-response analysis by inputting the worldwide available curves and estimated the site amplification. Barani *et al.* [2013] studied the effect of G/G_{max} and damping curve and concluded that the selection of curve has an influence in determining the site amplification. However, the less uncertain site-response study in specific cases is fundamentally dependent on

CONTACT P. Anbazhagan  anbazhagan2005@gmail.com  Department of Civil Engineering, Indian Institute of Science, Bangalore, India, 560012

Color versions of one or more of the figures in the article can be found online at www.tandfonline.com/ueqe.

 Supplemental data for this article can be accessed [here](#).

© 2019 Taylor & Francis Group, LLC

inclusion of representative soil property [Seed *et al.*, 1986; Bradley, 2011; Thompson *et al.*, 2012] and standardization of the numerical scheme used. Hence the identification of characteristic G/G_{max} and damping curves are of prime importance for any reliable site-response analysis.

Downhole array provides valuable data for evaluating the assumptions and capabilities of site-response analysis programs. Aydan *et al.* [2008] and Aydan [2015a, 2015b] have studied the ground motion of important earthquakes recorded in KiK-net stations. Various authors [Thompson *et al.*, 2012; Kaklamanos *et al.*, 2013, 2015] have used KiK-Net (Kiban-Kyoshin Network) for studying the different parameters and assumption in non-linear and equivalent linear total stress site-response. Anbazhagan *et al.* [2017] used the KiK-Net database for the identification of appropriate G/G_{max} and damping curve for rock, gravel and clay layers in the shallow bedrock sites. However, the study did not consider curves developed by Darendeli [2001] and Zhang *et al.* [2005], which were assumed to be suitable by Kaklamanos *et al.* [2015] for site-response analysis of KiK-Net sites. Akeju *et al.* [2017] explained the procedure for selecting and constructing the most appropriate curve for the normalized modulus reduction curve of soils.

This study aims at selecting the most representative shear modulus reduction and damping curve for deep as well as shallow sites having layers of rock, gravel, sand, and clay. Recorded ground motions are available at both bedrock and surface level with soil layering details in the KiK-Net database. Soil profiles have been further grouped based on the soil thickness and type. For the selected soil profiles, non-linear site-response analysis has been carried out using the pair of rock recorded ground motions as input. Predicted response spectra of the surface have been compared with the recorded surface spectra by considering the various available G/G_{max} and damping curve for all the four sites. Linear mixed-effect model has been used on residuals calculated from predicted and surface recorded amplification spectra. Determined bias and standard deviation for all the input curves have been compared and the best representative shear modulus reduction and damping curve has been suggested. G/G_{max} and damping curve suggested in this study can be used for the sites where no site-specific curves are available.

2. Ground Motions and Sites Selected for Analysis

The profiles used in this study have been obtained from the Kiban-Kyoshin network (KiK-Net, K-Net, <http://www.kyoshin.bosai.go.jp/>). The KiK-Net array consists of more than 1,000 observation stations, of which 700 have downhole and surface high-quality seismographs. Sites have been selected by considering Thompson *et al.* [2012] and Kaklamanos *et al.* [2013] studies, and database were obtained from KiK-net recorded station that has (1) the recorded ground motions with surface peak acceleration value greater than 0.05 g and (2) have at least 10 recorded motions where minimum signal to noise ratio is more than 5 for the 0.5–20 Hz passband. Selection criteria resulted in 580 ground motions for 23 deep soil profiles. Collected ground motions were processed as per the methodology proposed by Dawood *et al.* [2016], and a high-pass fourth-order acausal Butterworth filter was applied as per Boore and Bommer [2005] using the Boore Fortran Programs (TSSP). The corner frequencies were selected through the procedure given by Dawood *et al.* [2016], acquired from the corresponding NEES flat file for all the KiK-Net sites.

Thompson *et al.* [2012] used 100 sites with 4,862 ground motions recorded from 1,573 earthquakes with surface acceleration less than 0.1 g for studying the KiK-Net downhole array. Out of 100 sites, 16 were identified as suitable fit for one-dimensional (1D) horizontally polarized shear wave propagation (1D SH) and 53 were identified as poor fit for 1D SH assumption (LP). Out of 100 profiles used by Thompson *et al.* [2012], for only 16 profiles, the

depth of bedrock is more than 70 m as defined by Kaklamanos [2012]. Out of 16, only 15 profiles were considered as NGNH18 and was classified as HP site. Out of 15 profiles, 10 are classified as LP profiles [Thompson *et al.*, 2012]. Most of the profiles considered by Thompson *et al.* [2012] were either having sand or gravel as a predominant soil type, i.e., laying over a rock. Hence, another eight profiles having clay and silt as their predominant soil type are also selected in the present study. These profiles have low intra-event variability, therefore requires non-linear site-response analysis.

Out of 23 profiles, 10 profiles have clay/silt as a predominant soil type (e.g., AICH05, YMTH06). However, 10 and 16 profiles are having sand (e.g., SZOH42, KSRH04) and gravel (e.g., KMMH14, KSRH06) as predominant soil type, respectively. Minimum rock depth is available at 70 m depth (MIEH10), and maximum rock depth is available at 364 m depth (AICH05). Summary of all the sites considered in this study along with predominant type is given in Table 1.

Addition to deep profiles, shallow profiles are also considered for selecting the shear modulus reduction and damping curves. Four rock sites (i.e., IWTH05, FKSH18, IWTH08, IWTH27); one gravel site (i.e., FKSH11); and two sand sites (FKSH08, TCGH15) were considered as shallow profiles. Details of these sites are given in Anbazhagan *et al.* [2017]. Three clay predominant sites (IWTH02, SITH11, KSRH10) and two gravel predominant sites (FKSH11, IBRH18) are also considered, and detail of these sites can be referred from Yang *et al.* [2017]. Summary of these shallow sites is given in Table 2.

Thompson *et al.* [2012] observed the difference in V_s structure while comparing the V_s profiles determined through spectral analysis of surface waves and KiK-Net database. However, to address this issue, Monte Carlo simulations have been used for varying the V_s structure and comprehensive linear site response has been performed at LP sites using low amplitude ground motions (PGA~0.05 g). For all the simulated profiles, response spectra are obtained and compared with the geometric mean of the recorded response spectra at the top of the deposit. Pearson's correlation coefficient (R^2) is used in ranking the profiles. V_s profile which is comparable to the seed profile obtained from KiK-Net database and having high R^2 is considered further. Small strain damping values are varied in each layer of the simulated profiles obtained from Monte Carlo simulations. Like Kaklamanos *et al.* [2013], average small strain damping value for respective V_s profile is provided as the seed value of the small strain damping.

Numerous studies [e.g., Grelle and Guadagno, 2009] have found that P -wave velocity (V_p) of 1,000–2,000 m/s are characteristic of saturated soil. Hence, ground motion table is assumed where V_p first surpasses 1,500 m/s [Kaklamanos *et al.*, 2015]. The coefficient of lateral earth pressure at rest (K_o) is computed using the theoretical relationship between K_o and Poisson's ratio (ν), i.e., $K_o = \nu/(1 - \nu)$, where $\nu = \left(V_p^2 - 2V_s^2 \right) / \left(2V_p^2 - 2V_s^2 \right)$. Other model parameters used in this study are described further. In-situ density of each layer has been estimated using relationship developed by Anbazhagan *et al.* [2016] with $\pm 1\sigma$.

3. Methodology

Site-response analysis has been performed using DEEPSOIL [Hashash *et al.*, 2017]. Both equivalent linear total stress and non-linear analysis have been used for finally identifying shear wave velocity profiles. STRATA [Kottke *et al.*, 2018] has been used to perform linear site

Table 1 Description of deep soil profile used in this study.

S. no.	Site	Available soil type till Z_{BR}	Predominant soil type	Class as per Thompson <i>et al.</i> [2012]	Z_r	Z_{BR}	n	V_{30}	NEHRP site classification	Max PGA (g) at Z_r	Range of PGA (g) at surface
1	AICH05	Clay + sand	Clay	-	404.6	364	10	301	D	0.04	0.019–0.12
2	AOMH17	Sand + clay	Sand	-	117	74	23	378	C	0.08	0.04–0.29
3	EHH04	Sand + clay + gravel	Gravel	LP	200	94	10	254	C	0.14	0.01–0.32
4	IBRH17	Sand + silt + gravel	Sand + silt	LG	510	134	50	301	D	0.17	0.02–0.42
5	KMMH03	Rock	Rock	-	203	-	12	280	D	0.15	0.02–0.78
6	KMMH14	Gravel + rock	Gravel	-	113	83	50	248	D	0.15	0.04–0.45
7	KSRH05	Gravel + rock	Rock	LP	330	-	20	389	C	0.01	0.02–0.29
8	MIEH10	Silt + Gravel	Silt	-	197	70	10	422	C	0.33	0.02–0.85
9	SZOH42	Clay + Sand + Rock	Sand	LP	203	128	15	153	E	0.11	0.01–0.44
10	SZOH43	Silt + Sand	Sand	-	242	156	10	323	D	0.09	0.03–0.24
11	TCGH10	Gravel	Gravel	LP	132	100	50	371	C	0.20	0.02–0.60
12	TKCH08	Gravel	Gravel	LG	353	78	25	353	D	0.12	0.01–0.50
13	YMTH04	Gravel + Rock	Rock	-	103	-	14	248	D	0.03	0.02–0.22
14	YMTH06	Clay + Gravel	Clay	-	148	128	10	261	D	0.05	0.01–0.20
15	IWTH20	Gravel + Silt	Gravel	LP	156	92	21	289	D	0.19	0.03–0.40
16	IWTH24	Clay + Gravel	Clay	LP	150	99	20	486	C	0.21	0.04–0.50
17	KSRH04	Sand + Rock	Sand	LP	240	177	50	189	D	0.16	0.02–0.37
18	KSRH06	Gravel + Rock	Gravel	LG	237	115	20	326	D	0.21	0.04–0.75
19	KSRH07	Sand + Gravel + Rock	Sand + Rock	LG	222	187	20	204	D	0.24	0.03–0.57
20	NMRH04	Sand + Gravel + Rock	Sand + Gravel	LG	216	185	20	168	E	0.15	0.02–0.43
21	NMRH05	Gravel + Rock	Gravel	LP	220	185	15	209	D	0.13	0.03–0.39
22	TCGH12	Sand + Gravel	Gravel	LP	120	106	50	344	D	0.05	0.04–0.16
23	TCGH16	Clay + Gravel	Clay + Gravel	LP	112	88	55	213	D	0.17	0.05–1.19

Z_r : depth of downhole sensor (m); Z_{BR} : depth of bed rock (m); n : number of ground motion; V_{30} : time average shear wave velocity at top 30 m depth.

Table 2 Description of shallow soil profile used in this study.

S. no.	Site	Available soil type till Z_{BR}	Predominant soil type	Class as per Thompson <i>et al.</i> [2012]	Z_r	Z_{BR}	n	V_{s30}	NEHRP site classification	Max	Range of
										PGA (g) at Z_r	PGA (g) at surface
1	IWTH05	Rock	Rock	LP	103.3	–	20	429	C	0.17	0.09–0.81
2	FKSH18	Rock	Rock	LP	103	–	20	307	D	0.04	0.05–0.35
3	IWTH08	Rock	Rock	LG	103	–	20	305	D	0.04	0.03–0.37
4	IWTH27	Rock	Rock	LG	103	–	30	670	C	0.14	0.05–0.76
5	FKSH11	Gravel + Rock	Gravel	LG	118.2	35	20	240	D	0.12	0.02–0.27
6	IBRH18	Rock + Rock	Gravel	LP	504	32	50	559	C	0.15	0.03–0.60
7	NIGH12	Gravel + Rock	Gravel	LP	110	52	50	553	C	0.12	0.03–0.30
8	TCGH15	Sand + Rock	Sand	LP	300	21	50	423	C	0.07	0.04–0.34
9	FKSH08	Sand + Rock	Sand	LP	108	50	10	563	C	0.04	0.04–0.13
10	KSRH03	Sand + Rock	Sand	LP	107	33	15	250	D	0.15	0.05–0.80
11	SITH11	Clay + Rock	Clay	–	104	14	10	372	C	0.02	0.03–0.20
12	IWTH02	Clay + Rock	Clay	LG	102	15	20	390	C	0.04	0.04–1.09
13	KSRH10	Clay + Rock	Clay	LG	213	35	30	213	D	0.12	0.03–0.58

response and Monte Carlo trials for calibrating LP sites. The non-linear behavior of soil is captured through the pressure-dependent hyperbolic model for the backbone curve, developed by Konder and Zelasko [1963], modified by Matasovic [1993]. The unloading and reloading formulations are based on the extended Masing rules [Hashash *et al.*, 2017], and within boundary condition has been used. The shear modulus reduction and damping curves have been used to fit the modified hyperbolic model using the MRDF-UIUC procedure developed by Phillips and Hashash [2009]. Many authors including Hashash *et al.* [2010] and Stewart and Kwok [2009] have proposed modifications to the hyperbolic relationship to obtain reasonable estimates of shear strength post-fitting the model. Groholski *et al.* [2015] proposes a generalized quadratic/hyperbolic strength-controlled model to address this issue, and the module has been implemented in DEEPSOIL. This new constitutive model satisfies both the small strain and large strain modeling of the backbone curve of soils which exhibit strain-hardening behavior. This constitutive model was developed from fundamental principles of general quadratic equations considering a bounding behavior of an elastic-perfectly plastic response and resulting in a hyperbolic model. Detail regarding DEEPSOIL and model can be found in Hashash *et al.* [2017] and Groholski *et al.* [2015].

In the present study, the formulation proposed by Hashash *et al.* [2010] is used to obtain estimates of shear strength. Since, in downhole arrays, the static shear strength is not known beforehand, correlations between the shear wave velocity and undrained shear strength suggested by Dickenson [1994] are used. Frequency-independent Rayleigh damping is used to model the small strain damping as suggested by Phillips and Hashash [2009]. Dependence of overburden pressure on the behavior of the modulus reduction curve and small strain damping is modeled through two coefficients in DEEPSOIL.

For determining the goodness-of-fit for different G/G_{max} and damping curves, the observed response spectra at surface, $SA_{obs}(T)$ is compared with the predicted response spectra at surface, $SA_{pred}(T)$ from site-response study using DEEPSOIL. The residual between the observed and obtained SA (5% damping) is a natural logarithm space as:

$$SA_{resid}(T) = \ln[SA_{obs}(T)] - \ln[SA_{pred}(T)], \quad (1)$$

where the geometric mean is used to combine the two orthogonal horizontal components of the recorded ground motion. Negative and positive residuals, respectively, indicate

overpredictions and underpredictions. For properly acquiring the statistical significance of different G/G_{max} and damping curves, dependency between multiple recordings at single site need to be evaluated. Mixed-effect regression [Pineiro and Bates, 2000] is a statistical procedure that helps in evaluating the repeatable bias and variance when the data are grouped with one or more classification factors. Using mixed-effect regression models, the parameter at a specific spectral period, T can be modeled as:

$$SA_{resid}(T)_{i,j} = \alpha + \eta_{si} + \epsilon_{i,j} \quad (2)$$

here α is the population mean of $SA_{resid}(T)$, i.e., fixed effect, which represents the average bias in shear modulus and damping curves along with ground motions; η_{si} and $\epsilon_{i,j}$ are the inter-site and intra-site residuals, respectively. η_{si} and $\epsilon_{i,j}$, respectively, represent the deviation from the population mean of the mean residual for the i th site and deviation of ground motion observation j at site i from the mean residual at site i . Both inter, and intra-site residuals are normally distributed with zero mean random variable and τ_s and σ_o are respective standard deviations. This mixed-effect model was used in examining the precision and bias in G/G_{max} and damping curves used in site-response analysis. A typical flow chart explaining about the selection of these curves is illustrated as Fig. 1.

4. Overview of Shear Modulus Reduction and Damping Curves Used

Various researchers have developed several G/G_{max} and damping curve with different shear strain values and for different materials. For all the available G/G_{max} and damping curves for soil in the literature, a set of curves are widely used by researchers in site-response analysis. G/G_{max} and damping curves presented by Seed and Idriss [1970], Seed *et al.* [1986], Sun *et al.* [1988], Vucetic and Dobry [1991], EPRI [1993], Ishibashi and Zhang [1993], Rollins *et al.* [1998], Darendeli [2001], Menq [2003], Zhang *et al.* [2005, 2008], Kallioglou *et al.* [2008] and Chen *et al.* [2017] are widely used for describing the dynamic behavior of the soil column.

For site-response study of shallow profiles, the available G/G_{max} and damping curves in the literature do not require complex input parameters. However, in case of deeper soil profiles, various researchers [Hardin and Drnevich, 1972; Hashash and Park, 2001; Kokusho, 1980] acknowledged the effect of confining pressure on dynamic soil property, especially for granular profiles. Hashash and Park [2001] concluded the influence of pressure-dependent behavior is significant even for 100 m thick soil column, and larger amplitudes for shorter periods are observed in case of pressure-dependent model. Soil type, plasticity index (PI), mean effective confining stress (σ'_m), and strain (γ) have been reported as the most significant factors that affect the ratio of shear modulus by Zhang *et al.* [2005]. Other factors such as grain characteristics, over-consolidation ratio, frequency of loading, void ratio, and degree of saturation also effects G/G_{max} but the effect is not much significant [Darendeli, 2001; Zhang *et al.*, 2005]. However, σ'_m , γ , PI, soil type, number of loading cycles and frequency of loading are the most influencing factor for damping ratio (ξ).

Hence for the analysis, both pressure dependent and independent G/G_{max} and damping curves are used. In case of Rock, EPRI [1993], Schnabel [1973] and Choi [2008] are used (see Fig. E1). To study the non-linear behavior of gravel, Seed *et al.* [1986], Rollins *et al.* [1998], Roblee and Chiou [2004] and Menq [2003] are used (see Fig. E2). For evaluating the non-linear behavior of sand deposits, Darendeli [2001], Seed and Idriss [1984], Roblee and Chiou [2004], EPRI [1993] and Menq [2003] were used (see Fig. E3).

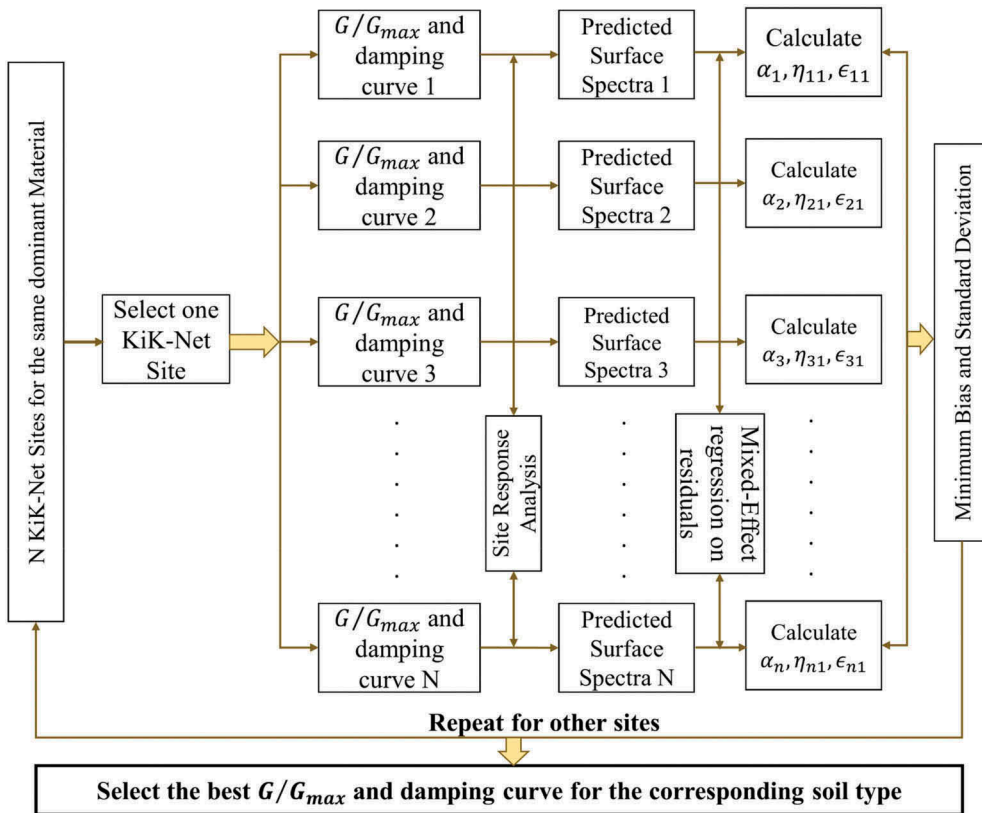


Figure 1. Flow chart showing the methodology used in selecting G/G_{max} and damping curve.

Vucetic and Dobry [1991], Yamada *et al.* [2008], Darendeli [2001], Roblee and Chiou [2004] are used for evaluating the non-linear behavior of clay deposits (see Fig. E4). The summary of the curves used in the analysis is given as an Electronic supplement.

5. Selection of Curves for Rock Sites

One pressure-dependent [i.e., EPRI, 1993] and two pressure-independent [i.e., Schnabel, 1973; Choi, 2008] and geology dependent [Zhang *et al.*, 2005] have been used to study the non-linear behavior of rock sites. The details of these sites used have been given in Tables 1 and 2. A typical plot of the variation of recorded and obtained response spectra for both shallow (i.e., IWTH05) and deep (i.e., KSRH05) rock predominant sites is given as Fig. 2a,b, respectively. The typical variation of residual (combined from all GMs) for different time periods considering all the recorded GMs for these two sites is given as Fig. 2c,d. Choi [2008] curves are significantly underpredicting the spectral acceleration values for different time periods, while Schnabel [1973] curves are overpredicting for longer time periods (see Fig. 2 (a)). However, in case of deep site (KSRH05), both Schnabel [1973] and Choi [2008] are overpredicting the spectral acceleration value for a particular GM. The presence of low V_s and density a weathered rock in case of KSRH05 till 100 m is the reason for overpredicting spectral acceleration instead of underpredicting as in case of IWTH05. This low-velocity rock is

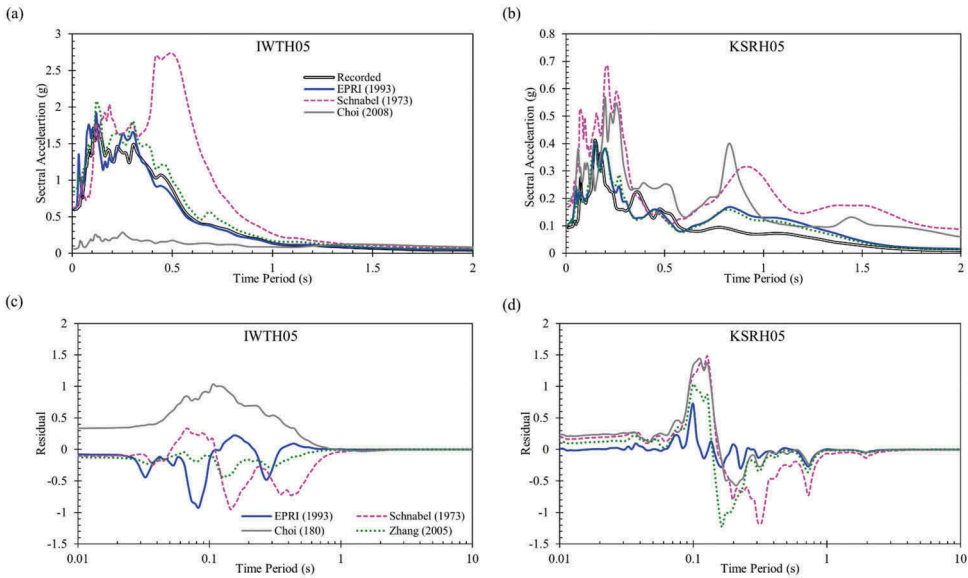


Figure 2. Variation of response spectra for different G/G_{max} and damping curve of (a) shallow site IWTH05 and (b) deep site KSRH05 and spectral (i.e., combined all GMs) residual for (c) shallow site IWTH05 and (d) deep site KSRH05.

further treated as gravel and residuals are compared. Bias in case of Zhang *et al.* [2005] curve is less as compared to EPRI [1993] (see Fig. 2c,d). The bias has been calculated in two ways: (a) using site as random variable and (b) using curve as random variable. In both the cases data is grouped according to residual calculated for different spectral periods. Using Equation 2, (a) fixed effect, α ; (b) intra-site/curve standard deviation, σ_o ; (c) inter-site/curve, τ_s ; and (d) total standard deviation, σ_Y have been calculated using the mixed-effect regression model.

The distribution of actual residuals and η_{si} for both site and curve is given in Fig. 3. Zhang *et al.* [2005] is performing better for (IWTH08 and FKSH18), whereas EPRI [1993] and Schnabel [1973] is having less bias value in case of both IWTH05 and IWTH27 (see Fig. 3). The residual values are more in case of Choi [2008] as compared to the other curves (see Fig. 3b). Presence of high shear wave velocity (V_s) within 5 m in case of IWTH27 may be the reason for pressure-independent Schnabel [1973] curves are performing better. However, based on the equivalent linear and non-linear analysis, Anbazhagan *et al.* [2017] suggested EPRI [1993] curves for site-response analysis in case of rock predominant sites. In the present study, Zhang *et al.* [2005] is having less bias as compared to EPRI [1993]. The fixed effect in case of Zhang *et al.* [2005] is -0.037 and EPRI [1993] is 0.0113 , i.e., the average ratio SA_{obs}/SA_{pred} for all the sites over the time periods, respectively, is 0.96 and 1.011 . However, based on the bias, it is difficult to conclude either Zhang *et al.* [2005] or EPRI [1993] or both the curves can be used in the case of rock sites. Hence, σ_o , τ_s , and σ_Y have been studied by considering sites as random variable. It can be seen that σ_Y in case of Zhang *et al.* [2005] is less as compared to EPRI [1993] (see Table 3).

Figs. 4 and 5 show the distribution of actual residuals and η_{si} for both site and curve, respectively, for deep sites. Zhang *et al.* [2005] curves are performing comparatively better for all the three sites (see Fig. 4a) and having less bias value. However, in case of KMMH03, all the

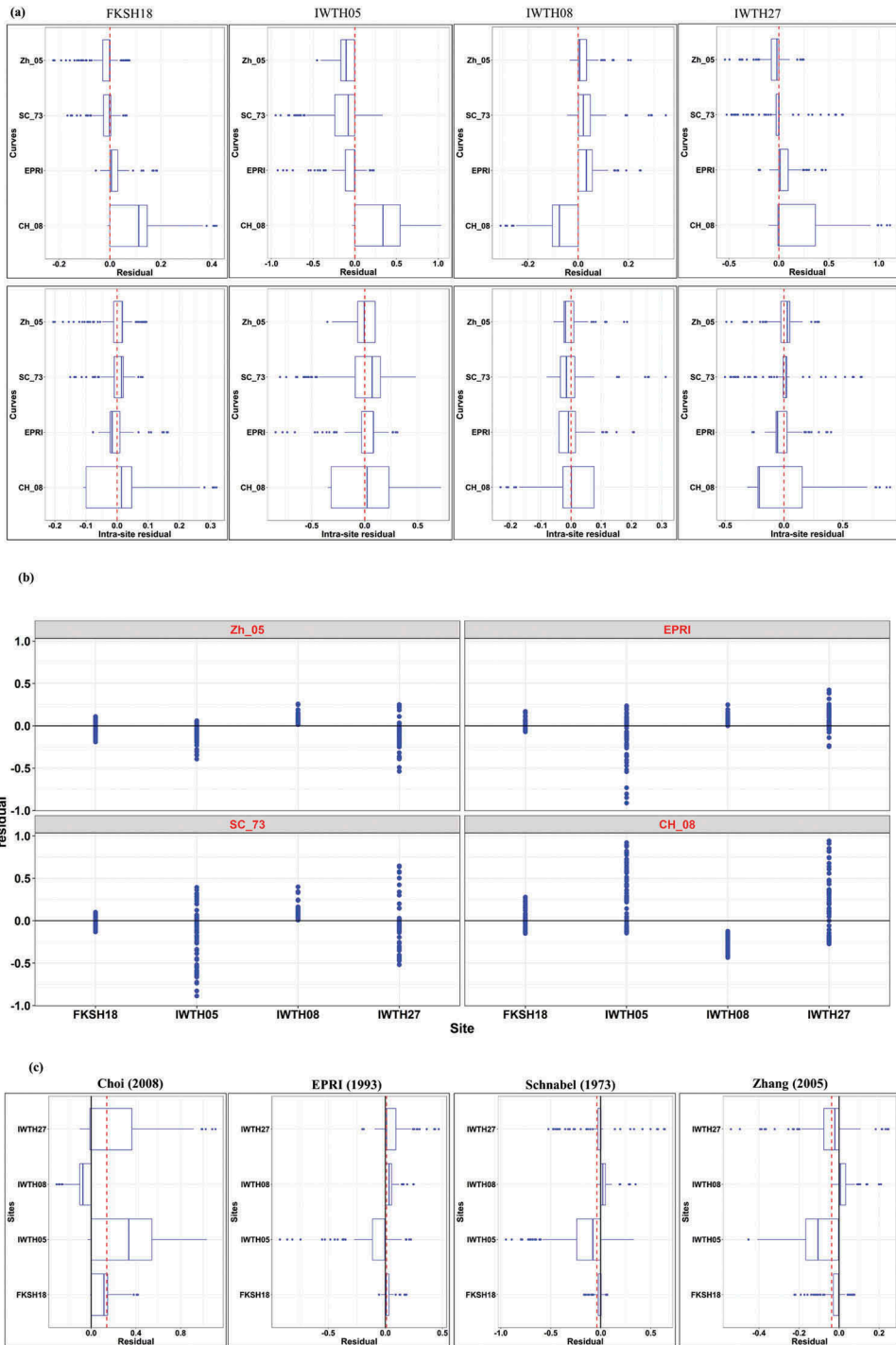


Figure 3. (a–c) Variation of actual residual for four shallow sites considering (a) curve and (b) site as random variable for all the time periods. Top of (a) is showing the bias and bottom is showing the intra-site residual for different curves used in the analysis of rock sites. (c) Variation of actual residuals considering sites as random variable. Red line indicates the fixed bias.

Table 3 Bias and standard deviation calculated using linear mixed-effect models for different curves. The numbers cited in the test is in square bracket.

Curves	Abbreviation	σ_o	τ_s	σ_y	a
Rock shallow soil profiles					
Schnabel [1973]	SC_73	0.0779	0.1729	0.1896	-0.0386
Choi [2008]	CH_08	0.2370	0.1670	0.2899	0.1390
EPRI	EPRI	0.0657	0.1206	0.1373	[0.0113]
Zhang <i>et al.</i> [2005]	ZH_05	0.0527	0.0907	0.1048	[-0.0370]
Rock deep soil profiles (using rock curves)					
Schnabel [1973]	SC_73	0.0225	0.2651	0.2660	0.0350
Choi [2008]	CH_08	0.0535	0.2712	0.2764	0.0995
EPRI	EPRI	0.0419	0.0857	0.0954	0.0279
Zhang <i>et al.</i> [2005]	ZH_05	0.0324	0.2033	0.2059	0.0298
Rock deep soil profiles (using gravel curves)					
Rollins <i>et al.</i> [1998] (LL)	R_LL	0.1322	0.2698	0.3004	0.0032
Rollins <i>et al.</i> [1998] (M)	R_M	0.0529	0.3246	0.3289	0.0581
Rollins <i>et al.</i> [1998] (UL)	R_UL	0.1605	0.3385	0.3746	0.0360
Seed <i>et al.</i> [1986]	S_86	0.1758	0.2885	0.3378	0.0829
Roblee and Chiou [2004]	RC_04	0.1206	0.2217	0.2524	0.0131
Zhang <i>et al.</i> [2005]	ZH_05	0.0324	0.2033	0.2059	0.0298
Menq [2003]	M_03	0.0010	0.4884	0.4884	0.0096
Gravel shallow soil profiles					
Rollins <i>et al.</i> [1998] (LL)	R_LL	0.0232	0.0644	0.0684	0.0167
Rollins <i>et al.</i> [1998] (M)	R_M	0.0299	0.0617	0.0686	0.0256
Rollins <i>et al.</i> [1998] (UL)	R_UL	0.0242	0.0534	0.0587	0.0273
Seed <i>et al.</i> [1986]	S_86	0.0310	0.0774	0.0834	0.0370
Roblee and Chiou [2004]	RC_04	0.0250	0.0587	0.0638	0.0220
Zhang <i>et al.</i> [2005]	ZH_05	0.0284	0.0698	0.0754	0.0317
Menq [2003]	M_03	0.0115	0.0435	0.0450	0.0100
Gravel deep soil profiles					
Rollins <i>et al.</i> [1998] (LL)	R_LL	0.1138	0.3513	0.3693	0.0913
Rollins <i>et al.</i> [1998] (M)	R_M	0.0342	0.3669	0.3685	0.0848
Rollins <i>et al.</i> [1998] (UL)	R_UL	0.1411	0.3726	[0.3984]	0.1510
Seed <i>et al.</i> [1986]	S_86	0.1140	0.3730	0.3900	0.1602
Roblee and Chiou [2004]	RC_04	0.0507	0.2626	0.2675	0.0139
Zhang <i>et al.</i> [2005]	ZH_05	0.0759	0.1711	0.1872	-0.0878
Menq [2003]	M_03	0.0001	0.0631	[0.0631]	-0.0013
Sand shallow soil profiles					
Darendeli [2001]	DA_01	0.0099	0.0270	[0.0288]	-0.0016
EPRI [1993]	EPRI	0.0083	0.0222	0.0237	-0.0011
Menq [2003]	M_03	0.0010	0.0191	[0.0191]	-0.0001
Roblee and Chiou [2004]	RC_04	0.0095	0.0209	0.0230	-0.0023
Seed and Idriss [1970] (LL)	SEI_L	0.0065	0.0245	0.0253	0.0005
Seed and Idriss [1970] (M)	SEI_M	0.0090	0.0237	0.0253	-0.0036
Seed and Idriss [1970] (UL)	SEI_U	0.0125	0.0256	0.0285	-0.0090
Zhang <i>et al.</i> [2005]	ZH_05	0.0069	0.0251	0.0260	-0.0055
Sand deep soil profiles					
Darendeli [2001]	DA_01	0.0840	0.1670	0.1869	0.0074
EPRI [1993]	EPRI	0.0513	0.1562	0.1644	-0.0604
Menq [2003]	M_03	0.0140	0.0762	0.0775	-0.0308
Roblee and Chiou [2004]	RC_04	0.0805	0.1312	0.1539	-0.0192
Seed and Idriss [1970] (LL)	SEI_L	0.0145	0.1988	0.1993	0.0148
Seed and Idriss [1970] (M)	SEI_M	0.0001	0.1708	0.1708	0.0746
Seed and Idriss [1970] (UL)	SEI_U	0.0171	0.2339	0.2345	0.0174
Zhang <i>et al.</i> [2005]	ZH_05	0.0010	0.0659	0.0659	-0.0079
Clay shallow soil profiles					
Darendeli [2001]	DA_01	0.0255	0.0601	0.0653	0.0081
Roblee and Chiou [2004]	RC_04	0.0176	0.1069	0.1083	0.0370
Vucetic and Dobry [1991]	VD_91	0.0271	0.1140	0.1172	0.0350
Yamada <i>et al.</i> [2008]	YA_08	0.0207	0.1178	0.1196	0.0498
Zhang <i>et al.</i> [2005]	ZH_05	0.0223	0.0801	0.0832	0.0137
Clay deep soil profiles					
Darendeli [2001]	DA_01	0.0533	0.1403	0.1501	0.1027
Roblee and Chiou [2004]	RC_04	0.0533	0.1403	0.1501	0.0428
Vucetic and Dobry [1991]	VD_91	0.0001	0.0808	0.0808	0.0206
Yamada <i>et al.</i> [2008]	YA_08	0.0517	0.1470	0.1558	0.0965
Zhang <i>et al.</i> [2005]	ZH_05	0.0196	0.0593	0.0624	0.0428

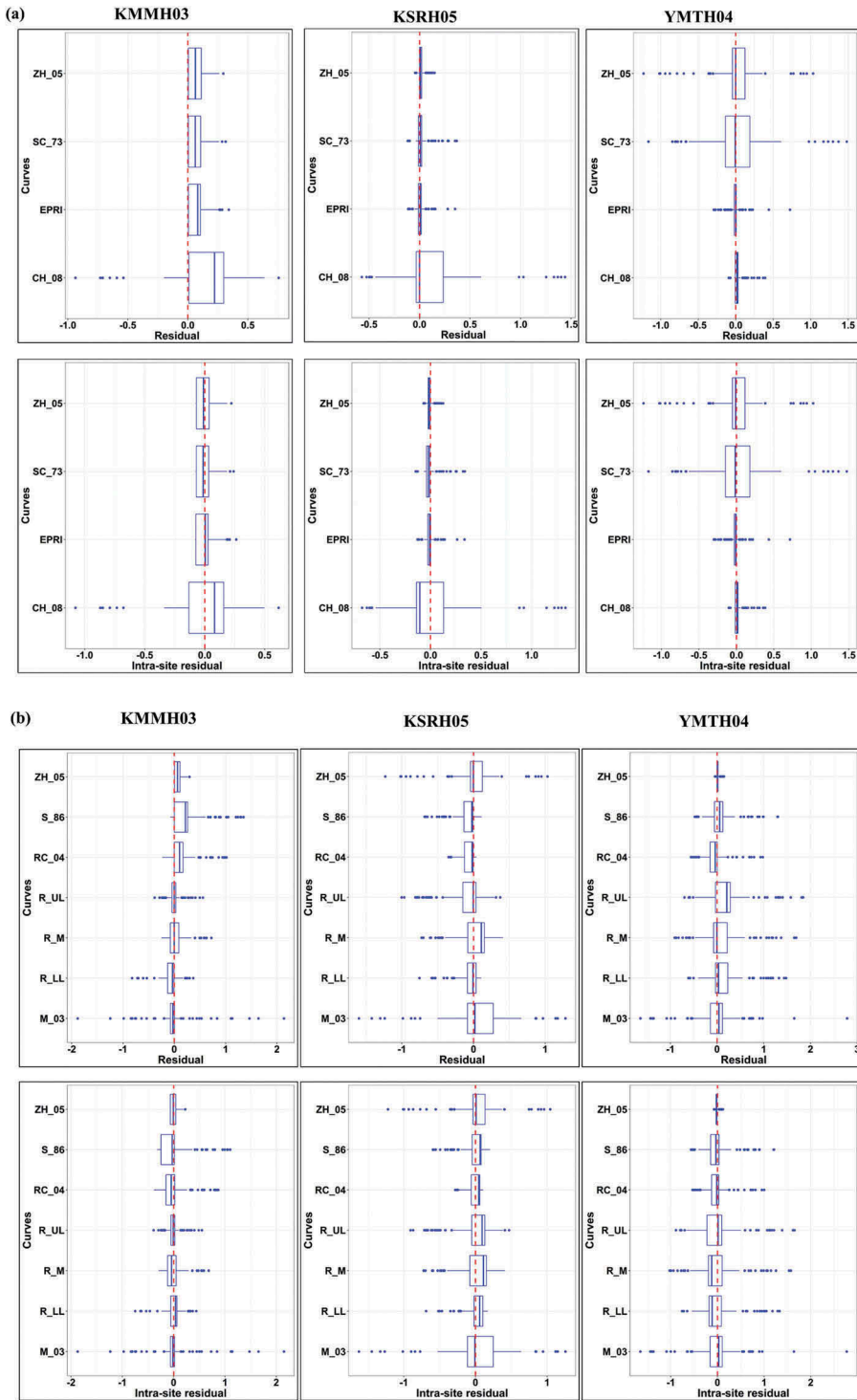


Figure 4. Variation of actual residual for three deep rock sites considering (a) rock specific curve and (b) gravel specific curve as random variable for all the time periods. Variation of residuals using (c) rock specific and (d) gravel specific curve considering site as random variable. Top of (a,b) is showing the bias and bottom is showing the intra-site residual for different curves used in the analysis of rock sites.

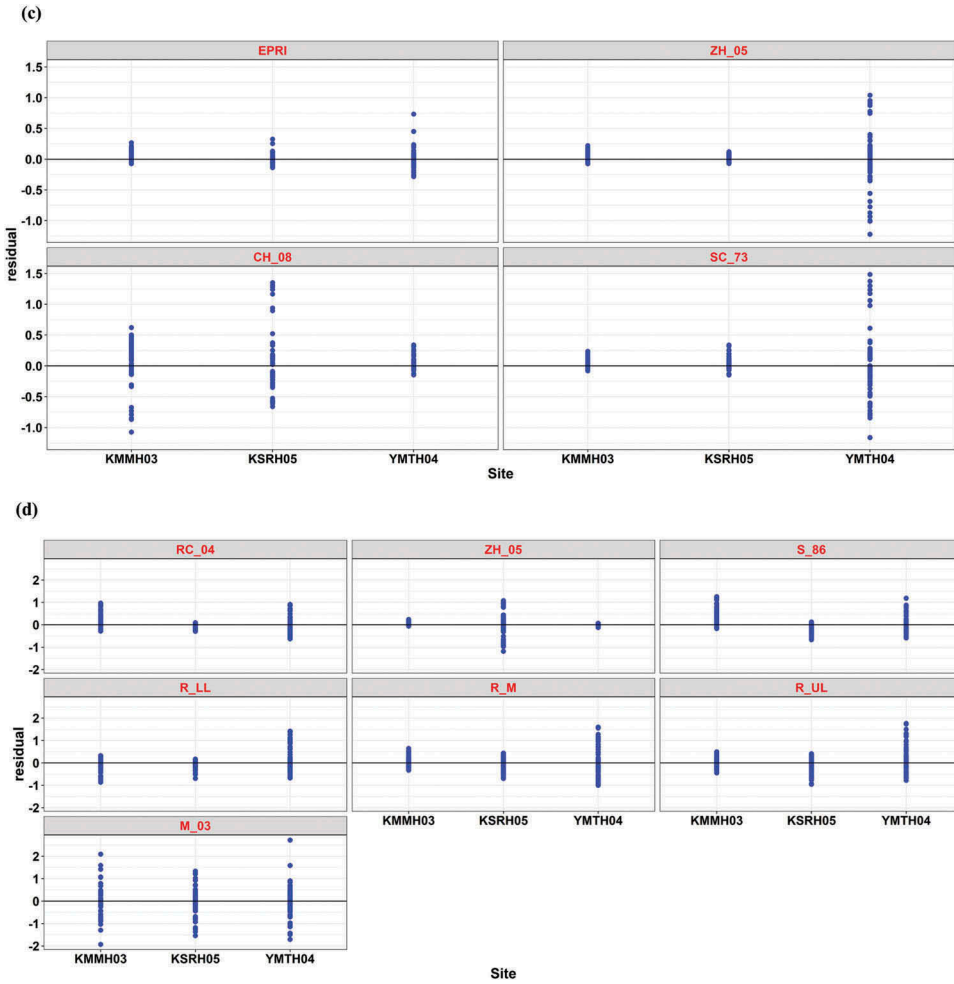


Figure 4. (Continued).

four curves are under predicting the spectral acceleration for all the time periods, which may be due to the sudden change in V_s value from 30 to 80 m. Choi [2008] and EPRI [1993] curves are predicting well in case of YMTH04, which may be due to the presence of low V_s mud tuff. However, Zhang *et al.* [2005], EPRI [1993] and Schnabel [1973] curves are performing well in case of KSRH05, which may be due to the constant high V_s layer within the first 50 m (i.e., less impedance ratio). Since concluding about the suitable curve is difficult, σ_o , τ_s , and σ_Y for all the spectral periods are also studied. It is observed that EPRI [1993] curves have less σ_Y as compared to other curves (see Table 2). In all the three profiles, low-velocity tuff and gravel are also present; hence, these profiles are also analyzed using the gravel curves. Based on the analysis, it is observed that Zhang *et al.* [2005] and Roblee and Chiou [2004] curves are performing better as compared to other gravel curves (see Fig. E2). Further, the standard deviation and bias with respect to different time periods have been studied. It is noted that the bias and total standard deviation value of EPRI [1993] curves are less as compared to Zhang *et al.* [2005] curves.

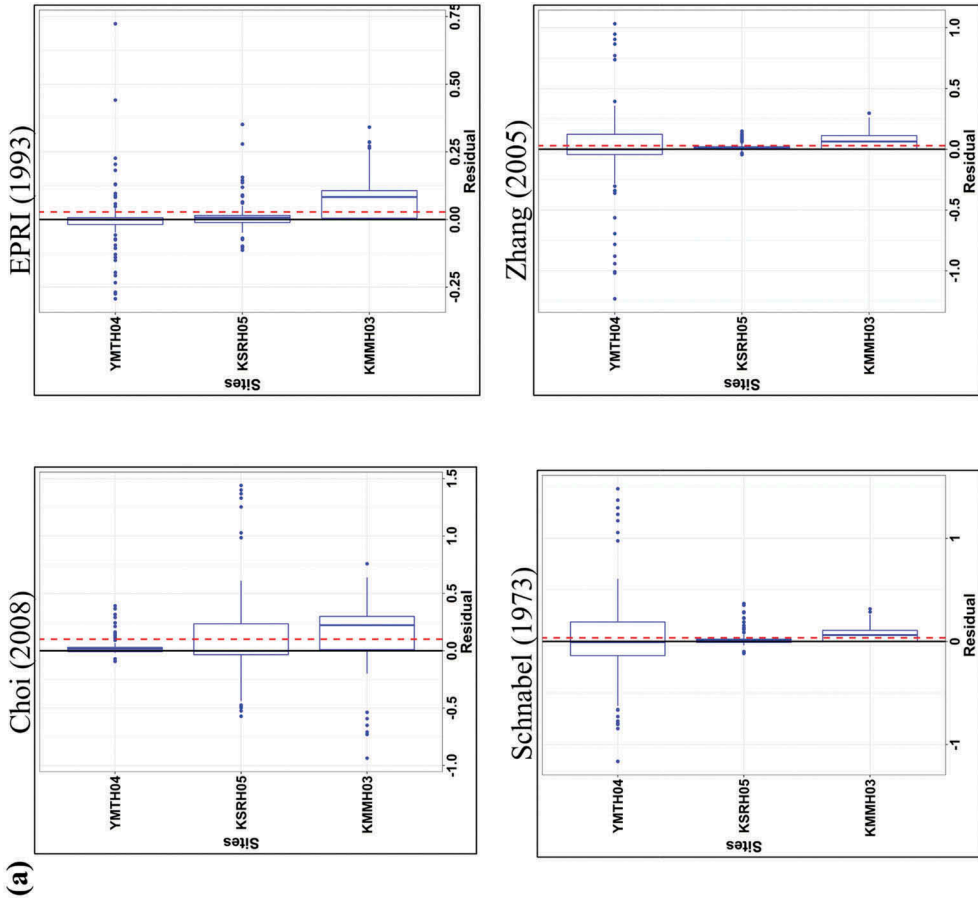


Figure 5. Variation of actual residuals using (a) rock and (b) gravel specific curve considering sites as random variable. Red line indicates the fixed bias.

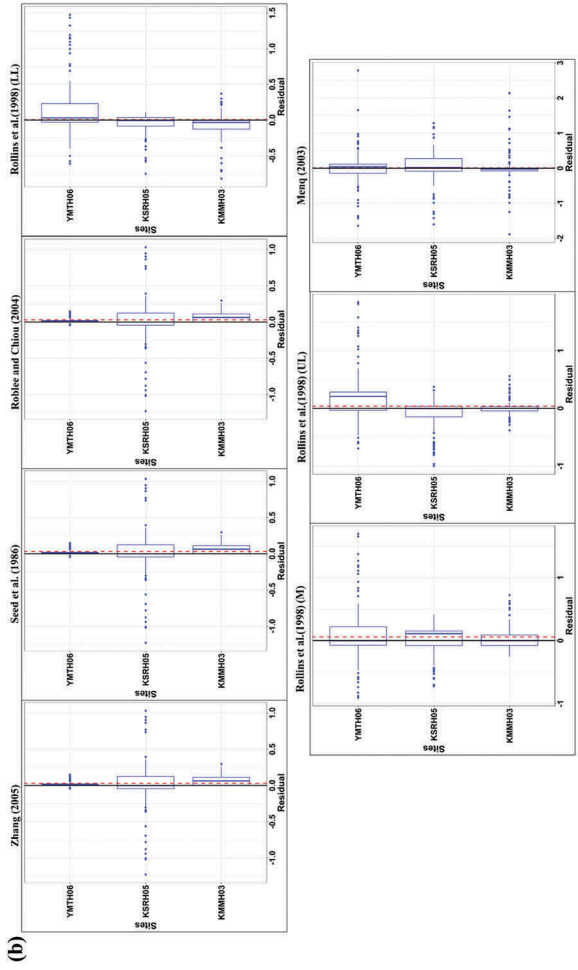


Figure 5. (Continued).

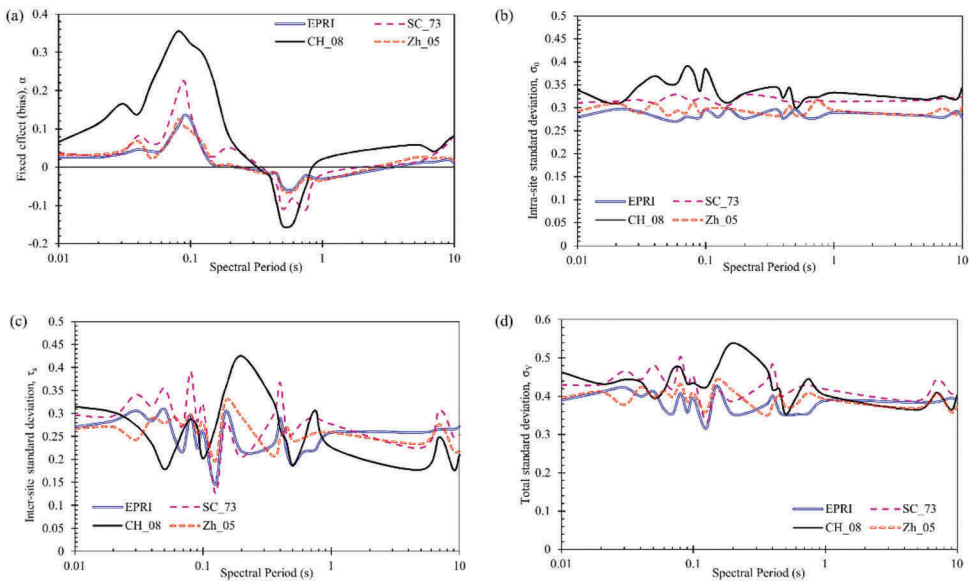


Figure 6. Period dependence of the parameters of the linear mixed-effects regression model for rock sites: (a) fixed effect, α ; (b) intra-site standard deviation, σ_0 ; (c) inter-site standard deviation, τ_s ; and (d) total standard deviation, σ_γ .

Fig. 6a shows the variation of average bias determined using a particular curve with spectral period. All the curves have positive bias (underprediction of ground motions) at spectra period less than 0.2 s. Except Choi [2008], all the three curves have almost zero bias for shorter spectral period and long periods, i.e., after 1 s. Bias in case of both Zhang *et al.* [2005] and EPRI [1993] curves is less as compared to Roblee and Chiou [2004] and Choi [2008] curves. Fig. 6b–d characterizes the variability of different curves residuals. For all the curves, intra-site standard deviation has been varied within the range of 0.25–0.35 natural log units and less erratic as compared to inter-site standard deviation, τ_s . The total standard deviation in case of EPRI [1993] is more constant as compared to the other three curves. However, major difference in all the curves is observed in fixed effect as compared to intra-site standard deviation.

Based on the overall analysis of both shallow as well as deep profiles, it can be suggested that if the geological age of the rock deposition is known then Zhang *et al.* [2005] curves can be used, else EPRI [1993]. Zhang *et al.* [2005] and EPRI [1993] curves are performing similarly in case of Quaternary deposits. However, EPRI [1993] curves are performing better in case of high-velocity rock deposition at deeper sites as compared to Zhang *et al.* [2005] curves. For deep sites, if tuff ($V_s \leq 300$ m/s) is present, Choi [2008] curves can also be used. Conclusively, for site-response analysis in case of rock predominant sites, EPRI [1993] and Zhang *et al.* [2005] curves can be used for rock sites, $V_s \geq 800$ m/s and $V_s < 800$ m/s, respectively, for Quaternary deposits.

6. Selection of Curves for Gravel Sites

For gravel, two pressure-independent [Seed *et al.*, 1986; Rollins *et al.*, 1998] and two overburden pressure dependent (i.e., Roblee and Chiou, 2004; Menq, 2003] and one geological

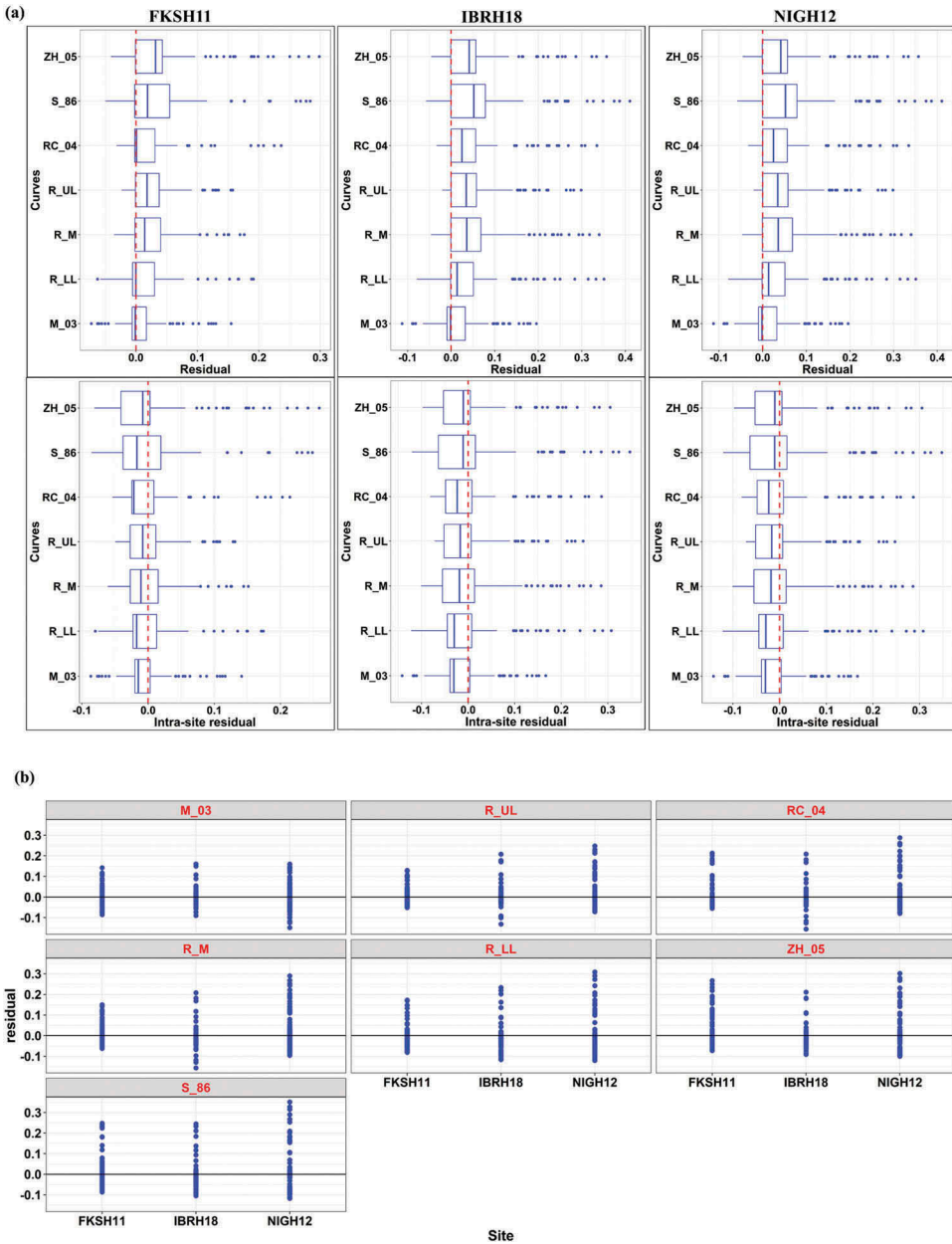


Figure 7. Variation of actual residual for three shallow gravel sites considering (a) curve and (b) site as random variable for all the time periods. Top of (a) is showing the bias and bottom is showing the intra-site residual for different curves used in the analysis of rock sites.

age-dependent [Zhang *et al.*, 2005] G/G_{max} and damping ratio curves have been used. The details of the gravel predominant sites used in the analysis are given in Tables 1 and 2.

Fig. 7a,b shows the variation of actual residuals considering curve and site as a random variable, respectively. Except for Menq [2003], rest all the four curves are under predicting the spectral acceleration values in case of NIGH12 and FKSH11. Whereas, in case of IBRH18, bias

is less for all the five curves. Calculated bias is identical in case of Rollins *et al.* [1998], Roblee and Chiou [2004] and Zhang *et al.* [2005] and minimum in case of Menq [2003] (see Fig. E6). Similarly, σ_Y is maximum in case of Seed *et al.* [1986] and minimum in case of Menq [2003] (see Table 3). For NIGH12 and FKSH11, significant difference is observed between calculated and observed spectral acceleration values between the period ranges of 0.08–0.14 s and 0.18–0.22 s. However, the bias is less in case of Menq [2003] for all the spectral periods as compared to other curves. Anbazhagan *et al.* [2017] concluded that Rollins *et al.* [1998] (-SD) and Roblee and Chiou [2004] curves can be used to define the non-linear behavior of the gravel predominant sites. However, in the present study, Menq [2003] curves are providing reliable estimate of ground response for all the spectral periods. The overall sigma in case of Menq [2003], Rollins *et al.* [1998] (-SD) and Roblee and Chiou [2004] is 0.066, 0.103, 0.09, respectively, while considering time periods as fixed and random variable.

Menq [2003] curves are having less bias value as compared to other curves, except in case of KMMH14, where Zhang *et al.* [2005] curves are having less bias value (see Fig. E7a,b). Zhang *et al.* [2005] curves are mostly underpredicting, and Seed *et al.* [1986] and Rollins *et al.* [1998] (UL) are overpredicting the SA values for all the spectral period range (see Fig. E8). σ_o is less in case of Rollins *et al.* [1998] (M) as compared to Zhang *et al.* [2005] and Roblee and Chiou [2004]. However, σ_Y is maximum in case of Rollins *et al.* [1998] (UL), i.e., 0.398 and minimum is case of Menq [2003], i.e., 0.063 (see Table 3).

All the curves have positive bias (underprediction of ground motions) except for the spectral period ranging from 0.15 to 0.35 (see Fig. 8a). All curves have almost zero bias for longer periods, i.e., after 1 s. Bias in case of Menq [2003] curves is less as compared to other curves, however, after 0.35 s, bias in the case of Zhang *et al.* [2005] and Menq [2003] curves is almost equal. Fig. 8b–d characterizes the variability of different curves residuals. Bias and standard deviation in case of

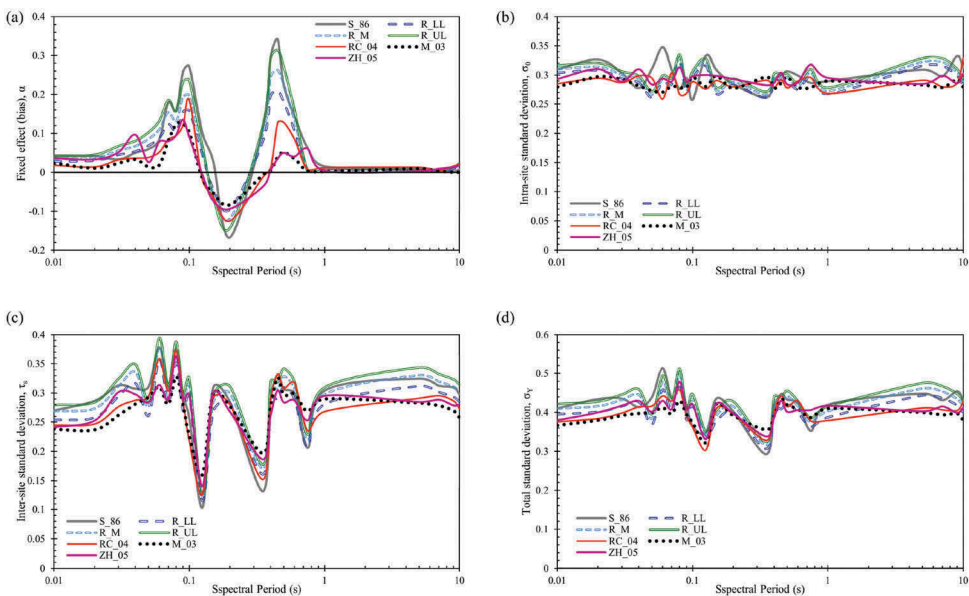


Figure 8. Period dependence of the parameters of the linear mixed-effects regression model for gravel sites: (a) fixed effect, a ; (b) intra-site standard deviation, σ_0 ; (c) inter-site standard deviation, τ_S ; and (d) total standard deviation, σ_Y .

Roblee and Chiou [2004] are not significantly different from Zhang *et al.* [2005]. For all the curves, intra-site standard deviation is varied within the range of 0.25–0.35 natural log units and less erratic as compared to inter-site standard deviation, τ_s . The total standard deviation of Menq [2003] is less as compared to the other three curves. However, the major difference in all the curve is observed in fixed effect as compared to intra-site standard deviation.

The reason for Menq [2003] curves having less bias and standard deviation value is because in addition to overburden pressure these curves are depending on the particle size as compared to Zhang *et al.* [2005] and Roblee and Chiou [2004]. Most of the available sites used in the analysis are a combination of gravel with either sand or clay or fine particles (e.g., TCGH10). Hence coefficient of uniformity (C_u) and median grain size (D_{50}) are important inputs in Menq [2003]. In this present study, which is varied based on density calculated and the type of soil available. For example, in case of TKCH08, D_{50} has been varied from 0.11 to 17.4 mm; and C_u from 1.1 to 15.9 and Menq [2003] curves are performing better than other curves with D_{50} ranged from 0.5 to 3 mm (increasing with density) and C_u from 1.1 to 5. Menq [2003] is performing better for $0.2 \leq D_{50} < 5$ and $1.1 \leq C_u < 10$ while considering all gravel profiles, based on the density of the deposition. However, in most of the cases, the value of D_{50} and C_u is not available. In such case, varying these values may not be workable, depending upon the project. Hence, bias and standard deviation have been calculated and compared for three curves, i.e., Menq [2003], Zhang *et al.* [2005], and Roblee and Chiou [2004] for both deep and shallow profiles. Significant variation is observed in bias value in all the three curves till 0.1 s, however, after 1 s no such variation in bias value is observed. In case of deep profiles, Zhang *et al.* [2005] is having less standard deviation, i.e., 0.112 as compared to Roblee and Chiou [2004], i.e., 0.201 while considering time periods as fixed variable.

Hence if the particle size is available, Menq [2003] curves can be used for gravel layers, otherwise Roblee and Chiou [2004] curves in case of shallow site and Zhang *et al.* [2005] curves for site-response analysis of deep gravel profiles.

7. Selection of Curves for Sand Sites

One pressure-independent [i.e., Seed and Idriss, 1984] and four pressure-dependent [Darendeli, 2001; Roblee and Chiou, 2004; EPRI, 1993; Menq, 2003] and one geological age-dependent [Zhang *et al.*, 2005] curves have been used for evaluating the non-linear behavior of sand deposits. In case of Darendeli [2001], over-consolidation ratio is reasonably assumed as unity, number of loading cycles and loading frequency are, respectively, assumed as 1 Hz and 10 [Darendeli, 2001; Kaklamanos *et al.*, 2015]. The details of these sites are given in Tables 1 and 2. Using mixed-effect models, α , σ_o , τ_s , and σ_Y have been calculated.

Menq [2003] and Zhang *et al.* [2005] curves are performing better for deep sites (see Fig. 9a,b). For most of the sites, EPRI [1993] curves are over predicting and Seed and Idriss [1970] (M) curves are under predicting the spectral acceleration values. Overall residuals are less in case of Menq [2003] and Zhang *et al.* [2005] and more in case of Seed and Idriss [1970]. Menq [2003] curves are performing better in case of AOMH17, SZOH43 and SZOH42. However, Zhang *et al.* [2005] curves are performing better in case of IBRH17, KSRH04, KSRH07 and NMRH04. In case of NMRH04, most of the curves are underpredicting except Zhang *et al.* [2005] which may be due to the presence of low-velocity soil deposition for deeper depth also. Fig. E9 shows the variation of actual residual and bias in all five G/G_{max} and damping ratio curves. The bias value is

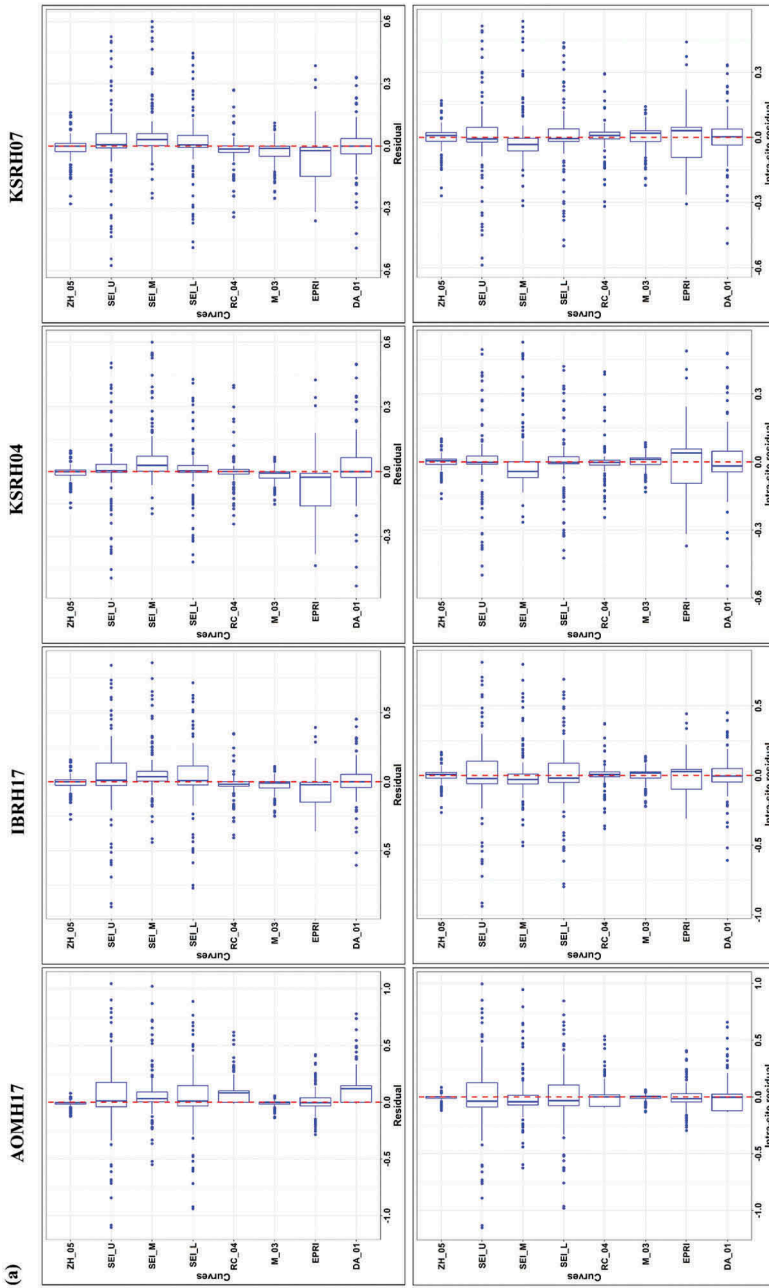


Figure 9. Variation of actual residuals for seven deep sites considering (a) curve and (b) site as random variable for all the time periods. Top of (a) is showing the bias and bottom is showing the intra-site residual for different curves used in the analysis of rock sites.

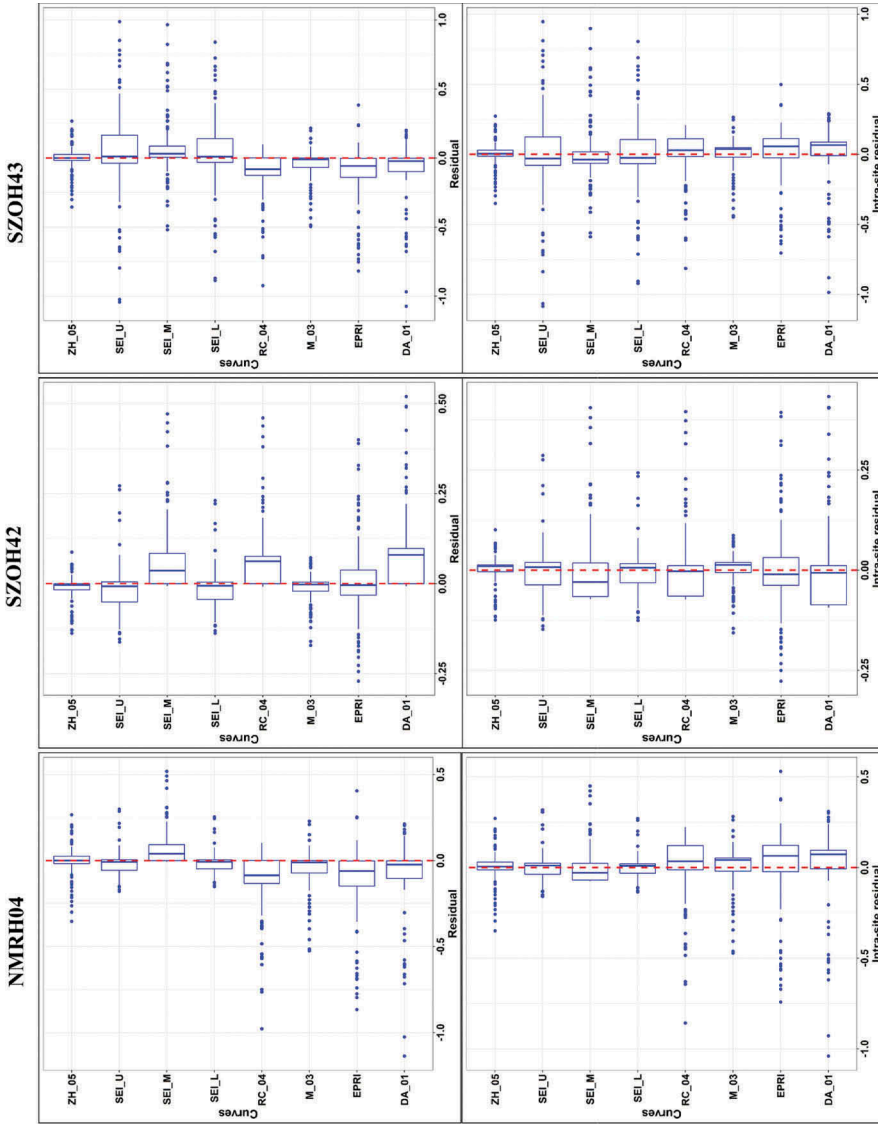


Figure 9 (Continued).

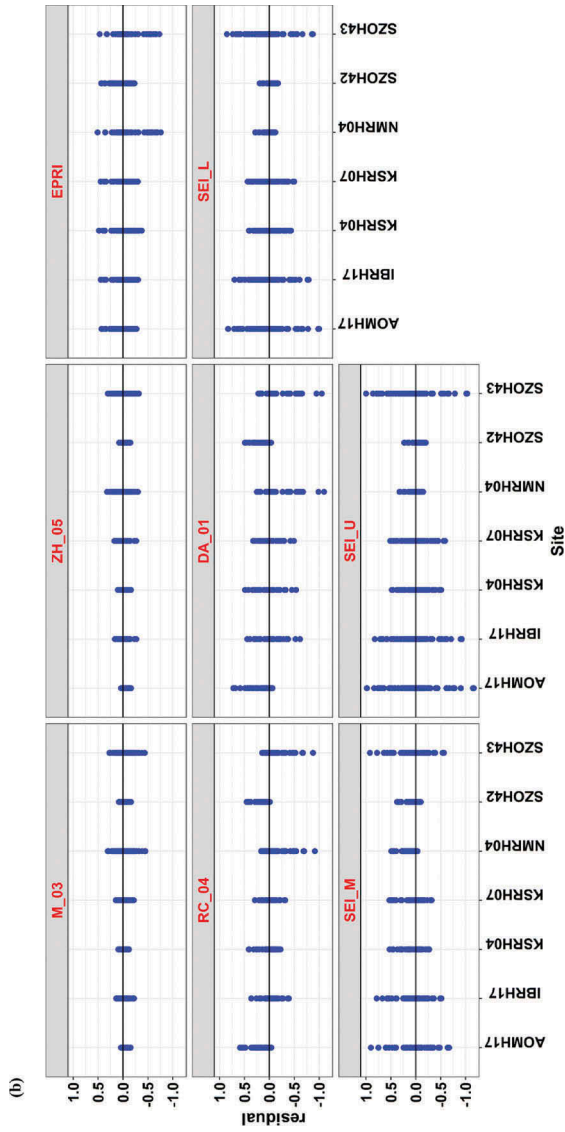


Figure 9 (Continued).

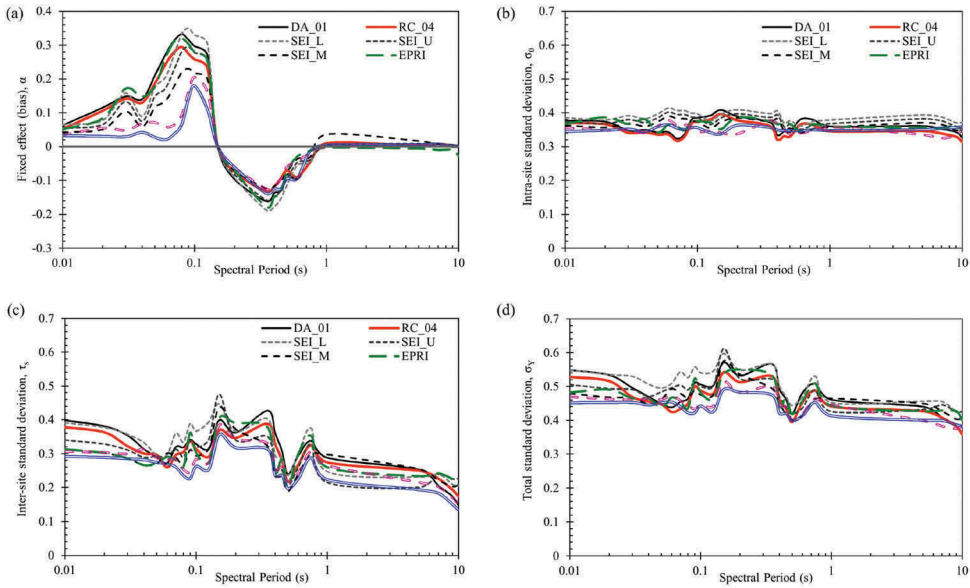


Figure 10. Period dependence of the parameters of the linear mixed-effects regression model for sand sites: (a) fixed effect, α ; (b) intra-site standard deviation, σ_0 ; (c) inter-site standard deviation, τ_S ; and (d) total standard deviation, σ_Y .

maximum for Seed and Idriss [1970] (M) and minimum for Zhang *et al.* [2005] curves. Negative bias is observed for Menq [2003] and EPRI [1993]. σ_Y is maximum (i.e., 0.23) in case of Seed and Idriss [1970] (UL) and Seed and Idriss [1970] (M) and minimum (i.e., 0.065) in case of Zhang *et al.* [2005] curves. Hence, Zhang *et al.* [2005] and Menq [2003] are performing better for sand deposits. Further bias value at different spectral periods have been studied for these five curves. Bias is less in case of Zhang *et al.* [2005] curves till 0.1 s and after 1.0 s both the curves have almost equal bias, tending toward zero. However, negative bias is observed for 0.08–0.14 s which may be due to not considering pore-pressure rise in the analysis.

Menq [2003] is performing better for all the three shallow sites and that may be due to the presence of sand-gravel mixture in all the sites (Fig. E10a,b). In case of FKSH08, except Menq [2003] and Zhang *et al.* [2005], almost all the curves are overpredicting bias values. Whereas KSRH03 and TCGH15 profiles are showing less bias for all the six curves. Bias value is almost zero expect for Zhang *et al.* [2005] and Seed and Idriss [1970] (UL) (see Fig. E11) curves. σ_Y is maximum (i.e., 0.028) in case of Darendeli [2001] and Seed and Idriss [1970] (UL) and minimum (i.e., 0.019) in case of Menq [2003] curves (see Table 3). It can be concluded that Menq [2003], Zhang *et al.* [2005] and Seed and Idriss [1970] (LL) are performing better in case of shallow sand deposits. Further bias value at different spectral periods is studied for these five curves. The overall sigma in case of EPRI [1993], Menq [2003], Seed and Idriss [1970] (LL), Seed and Idriss [1970] (UL) and Zhang *et al.* [2005] is 0.034, 0.028, 0.035, 0.032, 0.030, respectively, while considering time periods as fixed and random variable.

All the curves have positive bias (underprediction of ground motions) except for the spectral period ranging from 0.15 to 0.75 (Fig. 10a). All curves have almost zero bias for longer periods, i.e., after 1 s, except EPRI [1993] and Seed and Idriss [1970] (M) curves. Bias in case of Zhang *et al.* [2005] and Menq [2003] curves is less as compared to other curves. However, after 0.15 s,

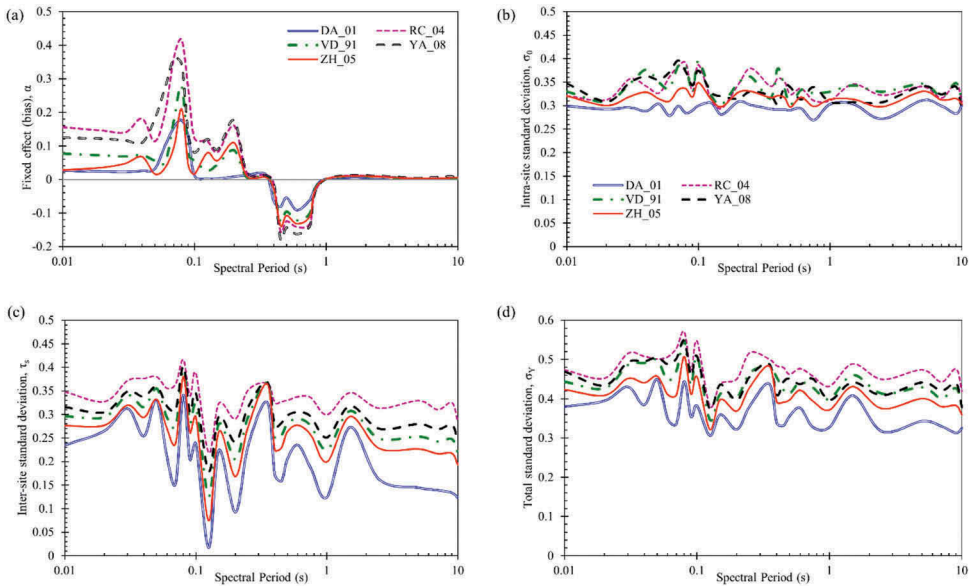


Figure 11. Period dependence of the parameters of the linear mixed-effects regression model for clay sites: (a) fixed effect, a ; (b) intra-site standard deviation, σ_0 ; (c) inter-site standard deviation, τ_5 and (d) total standard deviation, σ_γ .

bias in case of Zhang *et al.* [2005] and Menq [2003] is almost equal. Significant variability in bias value is observed for the short spectral period ranging from 0.03 to 0.1 s. Bias and standard deviation in case of Roblee and Chiou [2004] are not significantly different from Darendeli [2001] (see Fig. 10b–d). For all the curves, intra-site standard deviation is varying within the range of 0.30–0.40 natural log units and less erratic as compared to inter-site standard deviation, τ_5 . The total standard deviation of Zhang *et al.* [2005] is less as compared to the other curves and not significantly different from Menq [2003]. However, major difference in all the curves have been observed in fixed effect as compared to intra-site standard deviation.

Menq [2003] curves are performing better for the shallow profiles and Zhang *et al.* [2005] curves are performing better for deep soil deposits. However, if proper soil properties are not available instead of Menq [2003] either Zhang *et al.* [2005] or Roblee and Chiou [2004] can be used.

8. Selection of Curves for Clay and Silt Sites

Two pressure-independent curves [i.e., Vucetic and Dobry, 1991; Yamada *et al.*, 2008] and two pressure-dependent [i.e., Darendeli, 2001; Roblee and Chiou, 2004] curves have been used for evaluating the non-linear behavior of clay deposits along with Zhang *et al.* [2005]. The details of the sites considered are given in Tables 1 and 2.

All the clay curves are mostly dependent on soil plasticity. It is important to see the non-linear behavior of clay profiles with varying PI values. Hence, parametric study has been carried out to select the most representative PI values, so that the residual will be less between the observed and recorded SA at the surface. The PI value varies from 0 to 100 for all G/G_{max} and damping ratio curves for both shallow and deep profiles. For example, in case of KSRH10 for the first 35 m, PI

values vary from 0, 10, 15, 20, 30, 40, 50, 75, 100 for all the cases. Vucetic and Dobry [1991], Darendeli [2001], Zhang *et al.* [2005], and Yamada *et al.* [2008] curves are predicting less bias for PI range for $15 \leq PI < 20$, $40 \leq PI < 50$, $20 \leq PI < 30$ and $20 \leq PI < 30$, respectively. Similarly, in case of AICH05, Vucetic and Dobry [1991], Darendeli [2001], Zhang *et al.* [2005], and Yamada *et al.* [2008] curves are predicting less bias for PI range for $20 \leq PI < 30$, $50 \leq PI < 75$, $20 \leq PI < 40$ and $40 \leq PI < 50$, respectively. Among all the sites, curve having less bias for corresponding PI is selected for further site-response analysis and selection of proper curves. The selection of the best representative curves for clayey sites is explained further.

For KSRH10, all the curves are underpredicting the spectral acceleration values, even though bias in case of Zhang *et al.* [2005] is less as compared to other curves (see Fig. E12a, b). Darendeli [2001] curves are predicting better than all the curves and Zhang *et al.* [2005] curves are marginally better than Darendeli [2001]. Because of less clay depth in case of IWTH02 and SITH11, Vucetic and Dobry [1991] curves are showing less bias value. Bias is maximum in case of Yamada *et al.* [2008] (i.e., 0.049) and minimum in case of Darendeli [2001] curves (i.e., 0.008) (see Fig. E13). The total standard deviation in case of Vucetic and Dobry [1991] and Yamada *et al.* [2008] is 0.118 and 0.065 in case of Darendeli [2001].

Darendeli [2001] curves are predicting better in all the four profiles (see Fig. E14a,b). For IWTH24, TCGH16 and YMTH06, except Darendeli [2001], all the four curves are overpredicting the spectral acceleration values. The bias value is minimum in case of Darendeli [2001] (i.e., 0.042) and maximum for Yamada *et al.* [2008] and Roblee and Chiou [2004] (i.e., 0.112) (see Fig. E15). σ_Y is maximum in case of Yamada *et al.* [2008] and Roblee and Chiou [2004] (i.e., 0.151), and minimum in case of Darendeli [2001] (i.e., 0.061).

All the curves have positive bias (underprediction of ground motions) except for the spectral period ranging from 0.40 to 0.75 (see Fig. 11a). All curves have almost zero bias for longer periods, i.e., after 1 s. Bias in case of Darendeli [2001] is less as compared to other curves, however, after 1.0 s, bias in case of Zhang *et al.* [2005] and Darendeli [2001] curves is almost equal. Roblee and Chiou [2004] and Yamada *et al.* [2008] curves are significantly underpredicting the spectral acceleration values for spectral period range 0.05–0.25 s. This may be due to PI independency in case of Roblee and Chiou [2004] and overburden pressure-independency in case of Yamada *et al.* [2008]. Significant variability in bias value was observed for the short spectral period ranging from 0.01 to 0.1 s. Fig. 11b–d characterizes the variability of different curves residuals. Bias and standard deviation in case of Zhang *et al.* [2005] curves are not significantly different from Darendeli [2001] curves. For all the curves, intra-site standard deviation is varying within the range of 0.25–0.40 natural log units and less erratic as compared to inter-site standard deviation, τ_s . The total standard deviation of Darendeli [2001] curves is less as compared to the other curves and not significantly different from Zhang *et al.* [2005]. However, the major difference in all the curves is observed in fixed effect as compared to intra-site standard deviation.

Only Darendeli [2001] is available for silt sites. Hence, only one site (i.e., MIEH10) has been tested to find the suitable PI value. PI values vary as 0, 5, 10, 15, 20, 25, 30, 50. It can be seen that in case of $20 \leq PI < 30$, the bias value is less as compared to other PI value. At PI more than 30, there is a significant increase in bias and standard deviation value.

Hence, Darendeli [2001] and Zhang *et al.* [2005] curves are performing better in case of shallow profiles and Darendeli [2001] curves are performing better in case of deep soil deposits. Additionally, Darendeli [2001] curves are performing better for PI range 40–75 in case of deep

deposits and 30–50 in case of shallow clay deposits. For PI range from 20 to 30, Darendeli [2001] curves are representing better in case of silt deposits.

9. Limitation and Assumption of Current Study

In this study, non-linear 1D site-response model has been considered for selecting the representative curve for different soil types. As the grain size distribution is not available, hence, a qualitative estimate is used for soil classification. Sites are selected according to Thompson *et al.* [2012] based on poor and good fit for 1D wave propagation assumption, i.e., LP and LG sites. For LP sites, vertical incidence is not presumed as a source of error. The results derived from the present study may not be suitable for sites that are classified as HP and HG as per Thompson *et al.* [2012]. Difference in small strain damping ratio and shear wave velocity is used for attributing this error. Using the Monte Carlo simulations and linear 1D site-response analysis, shear wave velocity profiles have been estimated and used further in the analysis. Various developed shear modulus reduction and damping ratio curves demand different parameters which are difficult to obtain without soil sampling. Hence those curves are not used in the analysis. 1D site-response model that assumes horizontally polarized shear wave propagation assuming vertical incidence has been used for analysis. Due to lack of non-linear material data and pore-pressure data for KiK-net sites, complicated non-linear constitutive models could not be used. If the same selected curves are to be used for different sites other than Japanese sites, uncertainty must be taken into consideration. Additionally, it can be noted that these curves can only be used as an initial estimate to predict the surface amplification spectra for the sites where information about the soil deposit is not available.

10. Conclusion

This study aims at identifying and selecting shear modulus reduction and damping curves for the soils by dividing it into rock, gravel, sand, and clay part of KiK-Net downhole array network. 1D site-response analysis and Monte Carlo simulations are carried out for the sites which are not good for 1D wave propagation assumptions. Using the selected profiles, non-linear one-dimension total stress site-response analysis is carried out, by giving the rock recorded ground motions as input parameter. Both shallow and deep soil sites available are considered for selecting the representative G/G_{max} and damping ratio curves for the corresponding soil profile. Using the mixed-effect models, the residuals are calculated from recorded and predicted surface amplification spectra. Based on the results obtained, fixed effect bias and standard deviation, representing curves are selected. G/G_{max} and damping ratio curves given by Darendeli [2001] are found to perform better for PI range 40–75 in case of deep deposits, and 30–50 in case of shallow clay deposits. For PI range from 20 to 30, Darendeli [2001] curves represent better in case of silt deposits. G/G_{max} and damping ratio curves of Menq [2003] curves are found to perform better in case of shallow sites, and Zhang *et al.* [2005] curves are found to perform better in case of deep sites with dominant sand layers. Menq [2003] G/G_{max} and damping ratio curves are found to perform better in gravel dominated sites. In case of non-availability of proper soil sampling, G/G_{max} and damping ratio curves of Zhang *et al.* [2005] and Roblee and Chiou [2004] can be used for sand and gravel dominated sites. Limited G/G_{max} and damping ratio curves are available for rock sites, however, curves given by EPRI [1993] are found to be more suitable as compared to other curves available in the literature. For few gravel and sand

deposit profiles, pore-pressure rise and effective stress behavior significantly changes the pre-dominant period of soil columns. The recommended G/G_{max} and damping ratio curves can be used in the site-response analysis for the sites where site-specific curves are not available.

Acknowledgments

The authors would like to thank the two anonymous reviewers for giving their suggestions in improving the manuscript. The authors also wish to thank the National Research Institute for Earth Science and Disaster Resilience (NIED) and Kyoshin Net Strong Motion Network of Japan for providing an excellent earthquake database and valuable feedback for conducting this research.

Funding

The authors thank the Science and Engineering Research Board (SERB) of the Department of Science and Technology (DST), India for funding the project titled “Measurement of shear wave velocity at deep soil sites and site response studies,” Ref.: SERB/F/162/2015-2016.

References

- Akeju, O. V., Senetakis, K. and Wang, Y. [2017] “Bayesian parameter identification and model selection for normalized modulus reduction curves of soils,” *Journal of Earthquake Engineering*. doi:10.1080/13632469.2017.1323051.
- Anbazhagan, P., Prabhakaran, A., Madhura, H., Moustafa, S. S. R. and Al-Arifi, N. S. N. [2017] “Selection of representative shear modulus reduction and damping curves for rock, gravel and sand sites from the KiK-Net downhole array,” *Natural Hazards* **88**, 1741. doi:10.1007/s11069-017-2944-x.
- Anbazhagan, P. and Sitharam, T. G. [2008] “Seismic microzonation of Bangalore,” *Journal of Earth System Science* **117**, 833–852. doi:10.1007/s12040-008-0071-5.
- Anbazhagan, P., Uday, A., Moustafa, S. R. and Al-Arifi, S. N. [2016] “Correlation of densities with shear wave velocities and SPT N values,” *Journal of Geophysics and Engineering* **13**, 320. doi:10.1088/1742-2132/13/3/320.
- Aydan, Ö. [2015a] “Some considerations on a large landslide at the left bank of the Aratozawa Dam caused by the 2008 Iwate-Miyagi intraplate earthquake,” *Rock Mechanics and Rock Engineering, Special Issue on Deep-seated Landslides* **49**(6), 2525–2539. doi:10.1007/s00603-016-0977-1.
- Aydan, Ö. [2015b] “A critical testing of the applicability of some empirical relations used in the science and engineering of earthquakes through the 2011 Great East Japan Earthquake,” *Bulletin of Engineering Geology and the Environment* **74**(4), 1243–1254. doi:10.1007/s10064-014-0699-0.
- Aydan, Ö., Tokashiki, N. and Sugiura, K. [2008] “Characteristics of the 2007 Kameyama earthquake with some emphasis on unusually strong ground motions and the collapse of Kameyama Castle,” *Journal of the School of Marine Science and Technology* **6**, 83–105.
- Bakir, B. S., Sucuoğlu, H. and Yilmaz, T. [2002] “An overview of local site effects and the associated building damage in Adapazari during the 17 August 1999 Izmit earthquake,” *Bulletin of the Seismological Society of America* **92**, 509–526. doi:10.1785/0120000819.
- Barani, S., Ferrari, R. D. and Ferretti, G. [2013] “Influence of soil modeling uncertainties on site response,” *Earthquake Spectra* **29**(3), 705–732. doi:10.1193/1.4000159.
- Boore, D. M. and Bommer, J. J. [2005] “Processing of strong-motion accelerograms: needs, options and consequences,” *Soil Dynamics and Earthquake Engineering* **25**, 93–115. doi:10.1016/j.soildyn.2004.10.007.
- Bradley, B. A. [2011] “A framework for validation of seismic response analyses using seismometer array recordings,” *Soil Dynamics and Earthquake Engineering* **31**, 512–520. doi:10.1016/j.soildyn.2010.11.008.

- Bradley, B. A. and Cubrinovski, M. [2011] "Near-source strong ground motions observed in the 22 February 2011 Christchurch earthquake," *Seismological Research Letters* **82**, 853–865. doi:10.1785/gssrl.82.6.853.
- Chen, G., Zhou, Z., Sun, T., Wu, Q., Xu, L., Khoshnevisan, S. and Ling, D. [2017] "Shear modulus and damping ratio of sand-gravel mixtures over a wide strain range," *Journal of Earthquake Engineering*, 1–34. doi:10.1080/13632469.2017.1387200.
- Choi, W. K. [2008] "Dynamic properties of ash-flow tuffs," Ph.D. thesis, Department of Civil Engineering, University of Texas, Austin.
- Darendeli, M. B. [2001] "Development of a new family of normalized modulus reduction and material damping curves," Ph.D. dissertation, University of Texas at Austin, Austin.
- Dawood, H. M., Rodriguez-Marek, A., Bayless, J., Goulet, C. and Thompson, E. [2016] "A flatfile for the KiK-net database processed using an automated protocol," *Earthquake Spectra* **32**(2), 1281–1302. doi:10.1193/071214EQS106.
- Dickenson, S. E. [1994] "Dynamic response of soft and deep cohesive soils during the Loma Prieta earthquake of October 17, 1989," Ph.D. thesis, Department of Civil and Environmental Engineering, University of California, Berkeley. doi:10.3168/jds.S0022-0302(94)77044-2.
- Electric Power Research Institute (EPRI). [1993] "Guidelines for site specific ground motions," Palo Alto, CA, November. TR-102293.
- Grelle, G. and Guadagno, F. M. [2009] "Seismic refraction methodology for groundwater level determination: water seismic index," *Journal of Applied Geophysics* **68**, 301–320. doi:10.1016/j.jappgeo.2009.02.001.
- Groholski, D. R., Hashash, Y. M. A., Kim, B., Musgrove, M., Harmon, J. and Stewart, J. P. [2015] "Simplified model for small-strain nonlinearity and strength in 1-D seismic site response analysis," *Journal of Geotechnical and Geoenvironmental Engineering* **142**(9), 04016042. doi:10.1061/(ASCE)GT.1943-5606.0001496.
- Hardin, B. O. and Drnevich, V. P. [1972] "Shear modulus and damping in soils: design equations and curves," *Journal of the Soil Mechanics and Foundations Division, ASCE* **98**(7), 667–692.
- Hashash, Y. M. A., Musgrove, M. I., Harmon, J. A., Ilhan, O., Groholski, D. R., Phillips, C. A. and Park, D. [2017] *DEEPSOIL 7.0.5, User Manual*, Board of Trustees of University of Illinois at Urbana-Champaign, Urbana.
- Hashash, Y. M. A. and Park, D. [2001] "Non-linear one-dimensional seismic ground motion propagation in the Mississippi embayment," *Engineering Geology* **62**(1–3), 185–206.
- Hashash, Y. M. A., Phillips, C. and Groholski, D. R. [2010] "Recent advances in non-linear site response analysis," *Proc. of the 5th international conference on recent advances in geotechnical earthquake engineering and soil dynamics*, San Diego, California.
- Hough, S. E., Yong, A., Altidor, J. R., Anglade, D., Given, D. and Mildor, S.-L. [2011] "Site characterization and site response in Port-Au Prince, Haiti," *Earthquake Spectra* **27**, 137–155. doi:10.1193/1.3637947.
- Ishibashi, I. and Zhang, X. [1993] "Unified dynamic shear moduli and damping ratios of sand and clay," *Soils and Foundations* **33**(1), 182–191. doi:10.3208/sandf1972.33.182.
- Kaklamanos, J. [2012] "Quantifying uncertainty in earthquake site response models using the KiK-net database," Ph.D. dissertation, Tufts University, Medford, Massachusetts.
- Kaklamanos, J., Baise, L. G., Thompson, E. M. and Dorfmann, L. [2015] "Comparison of 1D linear, equivalent-linear, and nonlinear site response models at six KiK-net validation sites," *Soil Dynamics and Earthquake Engineering* **69**, 207–219. doi:10.1016/j.soildyn.2014.10.016.
- Kaklamanos, J., Bradley, B. A., Thompson, E. M. and Baise, L. G. [2013] "Critical parameters affecting bias and variability in site response analyses using KiK-net downhole array data," *Bulletin of the Seismological Society of America* **103**, 1733–1749. doi:10.1785/0120120166.
- Kallioglou, P., Tika, T. and Ptilakis, K. [2008] "Shear modulus and damping ratio of cohesive soils," *Journal of Earthquake Engineering* **12**(6), 879–913. doi:10.1080/13632460801888525.
- Karastathis, V. K., Papadopoulos, G. A., Novikova, T., Roumelioti, Z., Karmis, P. and Tsombos, P. [2010] "Prediction and evaluation of nonlinear site response with potentially liquefiable layers in the area of Nafplion (Peloponnesus, Greece) for a repeat of historical

- earthquakes,” *Natural Hazards and Earth System Sciences* **10**(11), 2281–2304. doi:10.5194/nhess-10-2281-2010.
- Kokusho, T. [1980] “Cyclic triaxial test of dynamic soil properties for wide strain range,” *Soils and Foundations* **20**, 45–60. doi:10.3208/sandf1972.20.2_45.
- Konder, R. L. and Zelasko, J. S. [1963] “A hyperbolic stress-strain formulation for sands,” *Proc. of 2nd Pan American conference on soil mechanics and foundation engineering*, Brazil, pp 289–324
- Kottke, A. R., Wang, X. and Rathje, E. L. [2018] “STRATA technical manual,” Department of Civil, Architectural, and Environmental Engineering, University of Texas, Austin.
- Kumar, A., Anbazhagan, P. and Sitharam, T. G. [2012] “Site specific ground response study of deep Indo-Gangetic basin using representative regional ground motion,” *Geo-Congress, State of art and practice in Geotechnical Engineering, Oakland California, Paper No. 1065*, pp 1888–1897. doi:10.1094/PDIS-11-11-0999-PDN.
- Mahajan, A. K., Sporry, R. J., Champati, P. K. R., Ranjan, R., et al. [2007] “Methodology for site response studies using multi-channel analysis of surface wave technique in Dehradun city,” *Current Science* **92**(7), 945–955.
- Matasovic, N. [1993] “Seismic response of composite horizontally-layered soil deposits,” Ph. D. thesis, University of California, Los Angeles.
- Menq, F. Y. [2003] “Dynamic properties of sandy and gravelly soils,” Ph.D. thesis, Department of Civil Engineering, University of Texas, Austin.
- Milne, J. [1898] *Seismology*, 1st ed, Kegan Paul, Trench, Truber, London.
- Phillips, C. and Hashash, Y. M. [2009] “Damping formulation for nonlinear 1D site response analyses,” *Soil Dynamics and Earthquake Engineering* **29**(7), 1143–1158. doi:10.1016/j.soildyn.2009.01.004.
- Pinheiro, J. C. and Bates, D. M. [2000] *Mixed-Effects Models in S and S-PLUS*, Springer-Verlag, New York, pp. 528.
- Roblee, C. and Chiou, B. [2004] “A proposed geindex model for design selection of non-linear properties for site response analyses,” *International workshop on uncertainties in nonlinear soil properties and their impact on modeling dynamic soil response*, PEER Headquarters, UC, Berkeley,
- Rollins, K., Evans, M. and Diehl, N. W. [1998] “Shear modulus and damping relationships for gravels,” *Journal of Geotechnical and Geoenvironmental Engineering* **124**(5), 396–405. doi:10.1061/(ASCE)1090-0241(1998)124:5(396).
- Schnabel, P. B. [1973] “Effects of local geology and distance from source on earthquake ground motions,” Ph.D. thesis, University of California, Berkeley.
- Seed, H., Wong, R., Idriss, I. and Tokimatsu, K. [1986] “Moduli and damping factors for dynamic analyses of cohesionless soils,” *Journal of Geotechnical Engineering* **112**(11), 1016–1032. doi:10.1061/(ASCE)0733-9410(1986)112:11(1016).
- Seed, H. B. and Idriss, I. M. [1970] “Soil moduli and damping factors for dynamic response analyses,” *Technical Report EERRC-70-10*, University of California, Berkeley
- Seed, H. B. and Idriss, I. M. [1984] *Ground Motions and Soil Liquefaction during Earthquake*, Earthquake Engineering Research Institute, Berkeley.
- Stewart, J. and Kwok, A. [2009] “Nonlinear seismic ground response analysis: protocols and verification against array data,” *PEER Annual Meet in San Francisco, Present 84*, Sacramento, California.
- Sun, J. I., Goleorkhi, R. and Seed, H. B. [1988] “Dynamic moduli and damping ratios for cohesive soils,” in *UCB/EERC-88/15* (Earthquake Engineering Research Center, University of California, Berkeley).
- Thompson, E. M., Baise, L. G., Tanaka, Y. and Kayen, R. E. [2012] “A taxonomy of site response complexity,” *Soil Dynamics and Earthquake Engineering* **41**, 32–43. doi:10.1016/j.soildyn.2012.04.005.
- Vucetic, M. and Dobry, R. [1991] “Effect of soil plasticity on cyclic response,” *Journal of Geotechnical Engineering* **117**(1), 89–107. doi:10.1061/(ASCE)0733-9410(1991)117:1(89).
- Yamada, S., Hyodo, M., Orense, R., Dinesh, S. V. and Hyodo, T. [2008] “Strain-dependent dynamic properties of remoulded sand-clay mixtures,” *Journal of Geotechnical and Geoenvironmental Engineering* **134**(7), 972–981. doi:10.1061/(ASCE)1090-0241(2008)134:7(972).

- Yang, Z., Yuan, J., Liu, J. and Han, B. [2017] "Shear modulus degradation curves of gravelly and clayey soils based on KiK-Net in situ seismic observations," *Journal of Geotechnical and Geoenvironmental Engineering* **143**, 06017008. doi:[10.1061/\(ASCE\)GT.1943-5606.0001738](https://doi.org/10.1061/(ASCE)GT.1943-5606.0001738).
- Zhang, J., Andrus, R. and Juang, C. H. [2005] "Normalized shear modulus and material damping ratio relationships," *Journal of Geotechnical and Geoenvironmental Engineering* **131**, 453–464. doi:[10.1061/\(ASCE\)1090-0241\(2005\)131:4\(453\)](https://doi.org/10.1061/(ASCE)1090-0241(2005)131:4(453)).
- Zhang, J., Andrus, R. and Juang, C. H. [2008] "Model uncertainty in normalized shear modulus and damping ratio Relationships," *Journal of Geotechnical and Geoenvironmental Engineering* **134**, 24–36. doi:[10.1061/\(ASCE\)1090-0241\(2008\)134:1\(24\)](https://doi.org/10.1061/(ASCE)1090-0241(2008)134:1(24)).